

# Tracing the History of Recent Bulge Star Formation in Active Galactic Nuclei

Xin Liu<sup>1\*</sup>

<sup>1</sup>*Department of Astrophysical Sciences, Princeton University, Peyton Hall – Ivy Lane, Princeton, NJ 08544*

Accepted 2010 May 12. Received 2010 May 11; in original form 2009 November 25

## ABSTRACT

We examine the relation between black hole accretion and bulge star formation as a function of look-back time ( $\tau$ ) in 20,541 obscured AGNs (with redshifts  $\bar{z} \sim 0.1$  and bolometric luminosities  $L_{\text{Bol}} \sim 10^{43}\text{--}10^{45}$  erg s<sup>−1</sup>) optically selected from the Sloan Digital Sky Survey (SDSS). To quantify the most recently formed stars with ages less than typical AGN lifetimes, we estimate the differentiated specific star formation rate (SSFR <sub>$\tau$</sub> ) based on population synthesis analysis. Eddington ratio ( $\lambda$ ) is inferred using [O III]  $\lambda 5007$  luminosity and stellar velocity dispersion as proxies for  $L_{\text{Bol}}$  and black hole mass respectively. We find that when  $\tau < \tau_0$ , SDSS AGNs follow a power law  $\lambda \propto \text{SSFR}_{\tau}^{1.0\text{--}1.1}$ ; the relation flattens out when  $\tau > \tau_0$ . The threshold timescale  $\tau_0$  is  $\sim 0.1$  ( $\sim 1$ ) Gyr in young (old) bulges. The scatter in the power laws is dominated by observational uncertainties. These results may provide useful constraints on models explaining the correlations between AGN activity and bulge star formation.

**Key words:** galaxies: active — galaxies: evolution — galaxies: nuclei — galaxies: starburst — galaxies: stellar content.

## 1 INTRODUCTION

The growth of supermassive black holes (SMBHs) could be linked with star formation (SF) in their host-galaxy bulges through multiple processes (see e.g., Heckman 2009, for a review). Stars form under the cosmological infall of gas (Binney 1977; Rees & Ostriker 1977), some of which could be accreted by central SMBHs (e.g., Burkert & Silk 2001). Galaxy mergers or interactions may trigger starburst and quasar activity (e.g., Sanders et al. 1988; Moore et al. 1996), which could output energy and momentum regulating further growth (e.g., Silk & Rees 1998; Fabian 1999; Springel et al. 2005). AGN-driven outflows could boost starbursts (e.g., Begelman & Cioffi 1989; Silk & Norman 2009). After being active, evolved stars may fuel AGNs via mass losses (e.g., Norman & Scoville 1988; Ciotti & Ostriker 1997). These processes may have different significance in regulating SMBH growth and bulge SF in various AGN populations at different cosmic epochs.

While post-starburst populations have been extensively observed in quasars (e.g., Boroson & Oke 1982; Canalizo & Stockton 2000; Jahnke et al. 2007; Liu et al. 2009) and in higher-luminosity AGNs (e.g., Kauffmann et al. 2003; Heckman et al. 2004; Cid Fernandes et al. 2004; Netzer 2009), the physical connection is still in debate. Two useful parameters are

specific star formation rate (SSFR  $\equiv \text{SFR}/M_*$ ) and Eddington ratio ( $\lambda \equiv L_{\text{Bol}}/L_{\text{Edd}}$ ). By studying the  $\lambda$  distribution in AGNs as a function of mean stellar age, Kauffmann & Heckman (2009) suggested that local AGNs occupy two distinct growth regimes. These authors used the 4000-Å break ( $D_n(4000)$ ; Bruzual 1983; Balogh et al. 1999) to characterize mean stellar age. Arising from a series of metallic lines,  $D_n(4000)$  is most sensitive to 1–2 Gyr old stars (e.g., Bruzual & Charlot 2003), whereas luminous AGN phases appear to be brief ( $< 0.1$  Gyr; e.g., Yu & Tremaine 2002).

To get higher temporal resolution and to quantify the most recently formed stars with ages less than typical AGN lifetimes, we examine SSFR averaged in the past  $\tau$  years (SSFR <sub>$\tau$</sub> ) based on population synthesis analysis (e.g., Bica 1988; Cid Fernandes et al. 2005; Asari et al. 2007). Under the multiple-starburst approximation, the differentiated SF histories in a statistical sample of AGNs offered by the Sloan Digital Sky Survey (SDSS; York, et al. 2000) enable us to investigate the correlation between AGN and recent bulge SF activity as a function of look-back time. This approach offers insights otherwise unattainable with single and older age indicators. We describe the AGN sample and the assumptions in estimating  $\lambda$  and SSFR <sub>$\tau$</sub>  along with uncertainties and selection biases in §2. §3 focuses on the correlations between  $\lambda$  and SSFR <sub>$\tau$</sub>  as a function of  $\tau$ . We discuss implications and caveats in §4. A cosmology with  $\Omega_m = 0.3$ ,  $\Omega_\Lambda = 0.7$ , and  $h = 0.7$  is assumed throughout.

\* E-mail: xinliu@astro.princeton.edu

## 2 DATA AND METHODOLOGY

### 2.1 The AGN Sample

The AGNs in this study were drawn from the MPA SDSS-DR4 type 2 AGN catalog (Kauffmann et al. 2003; Brinchmann et al. 2004). Type 2 AGNs are thought to be the obscured counterparts of type 1 AGNs according to unification models (e.g., Antonucci 1993; Urry & Padovani 1995). The parent sample was selected from SDSS emission-line galaxies at  $z < 0.3$  based on diagnostic line ratios that distinguish AGN from stellar ionizations (Baldwin et al. 1981). The four relevant lines ( $H\beta$ ,  $[\text{O III}] \lambda 5007$ ,  $H\alpha$ , and  $[\text{N II}] \lambda 6584$ ) were detected with signal to noise ratios  $(S/N) > 3$ . We adopt the empirical criterion,  $\log([\text{O III}] \lambda 5007/H\beta) > 0.61/(\{\log([\text{N II}] \lambda 6584/H\alpha) - 0.05\} + 1.3)$ , which separates AGNs from star-forming galaxies (Kauffmann et al. 2003). The analysis is limited to  $[\text{O III}] \lambda 5007$  luminosity  $L_{[\text{O III}]}$  in the range of  $10^{6.5} - 10^{8.5} L_{\odot}$  which corresponds to bolometric luminosities  $L_{\text{Bol}} \sim 10^{43} - 10^{45} \text{ erg s}^{-1}$  (e.g., Heckman et al. 2004; Reyes et al. 2008; Liu et al. 2009). The lower bound is to avoid faint-end incompleteness in a flux limited sample; It also effectively excludes low ionization objects. The upper bound is to avoid substantial scattered-AGN contamination (Zakamska et al. 2006; Liu et al. 2009; Greene et al. 2009), which makes population analysis more complicated and uncertain. Results on the  $L_{[\text{O III}]} > 10^{8.5} L_{\odot}$  objects will be presented elsewhere. The resulting sample consists of 20,541 objects with a median redshift of 0.1. These include 11,266 AGN-dominated objects with  $\log([\text{O III}] \lambda 5007/H\beta) > 0.61/(\{\log([\text{N II}] \lambda 6584/H\alpha) - 0.47\} + 1.19)$  above the theoretical “starburst limit” (Kewley et al. 2001) and 9,275 starburst-AGN composites<sup>1</sup>.

### 2.2 Bolometric Luminosity and Black Hole Mass

We use  $L_{[\text{O III}]}$  (from the MPA catalog, uncorrected for extinction<sup>2</sup>) to infer intrinsic AGN luminosity.  $L_{[\text{O III}]}$  is observed to be correlated with broad-band continuum luminosities in unobscured AGNs (e.g. Kauffmann et al. 2003; Reyes et al. 2008), despite having a significant scatter (e.g.,  $\sim 0.36$  dex in  $\log L_{[\text{O III}]}$  in the correlation with  $M_{2500}$  Reyes et al. 2008). We adopt the conversion  $\log(L_{\text{Bol}}/L_{\odot}) = 0.99 \times \log(L_{[\text{O III}]} / L_{\odot}) + 3.5 (\pm 0.5)$  appropriate for  $L_{[\text{O III}]}$  before extinction correction (Liu et al. 2009). We correct  $L_{[\text{O III}]}$  for the contribution from star formation using an empirical method based on an object’s position on the  $[\text{N II}]/H\alpha$  vs  $[\text{O III}]/H\beta$  diagram following Kauffmann & Heckman (2009). SMBH mass is estimated ( $M_{\text{BH}}$ ) from stellar velocity dispersion ( $\sigma_*$ ), assuming the relation observed in local inactive galaxies (e.g., Gebhardt et al. 2000; Ferrarese & Merritt 2000) calibrated by Tremaine et al. (2002). We adopt  $\sigma_*$

from the SDSS specBS pipeline (Adelman-McCarthy, et al. 2008) and exclude uncertain  $\sigma_*$  measurements ( $< 10$  or  $> 600 \text{ km s}^{-1}$ ).

### 2.3 Differentiated Specific Star Formation Rate

The common emission-line SFR indicators cannot be directly applied to luminous AGNs due to AGN contamination. Continuum indices are adopted such as  $D_n(4000)$  (e.g., Kauffmann et al. 2003; Brinchmann et al. 2004). To achieve higher temporal resolution than  $D_n(4000)$ , we estimate SSFR averaged in the past  $\tau$  years ( $\text{SSFR}_{\tau}$ ) from population synthesis analysis (e.g., Bica 1988; Cid Fernandes et al. 2005). Compared to SFR, SSFR is less subject to absolute calibration uncertainties associated with fiber effects and extinction (e.g., Brinchmann et al. 2004). We measure SSFRs inside the SDSS 3'' fibers (corresponding to the central  $\sim 1.5$  kpc at typical redshift of the sample) to quantify the bulge SF.

We adopt continuum models from the MPA DR4 archive (Tremonti et al. 2004), and have tested them on a randomly drawn subsample with our code (Liu et al. 2009). The assumption is that the bulk stellar population was built up in multiple starburst events with ages smaller than the age of the universe at the galaxy redshift. To sample the whole history of a host galaxy, stellar continuum is fit as a linear combination of ten instantaneous starburst models (broadened with the measured  $\sigma_*$ ) with ages of 0.005, 0.025, 0.10, 0.29, 0.64, 0.90, 1.4, 2.5, 5.0, and 11 Gyr (Bruzual & Charlot 2003), along with dust attenuation as an additional parameter. There are three sets of models with different metallicities (0.2, 1.0, and 2.5 solar). We adopt the metallicity with the smallest  $\chi^2$  as the best estimate. Given a best-fit model,  $\text{SSFR}_{\tau}$  is calculated as the summed ratio of the mass and age of the starburst templates that fall in interval  $\tau$ , divided by the total mass contained in all templates. The model coefficients in the MPA DR4 archive are in terms of luminosity<sup>3</sup>, and need to be converted to *mass* weights using the mass-to-light ratios of the starburst models from Bruzual & Charlot (2003).

We study the relation between AGN activity and recent bulge SF over three characteristic time intervals. First we divide the sample into young and old bulges, because the distribution of mean stellar age is bimodal (Kauffmann & Heckman 2009). For “young” bulges ( $D_n(4000) < 1.6$ )<sup>4</sup>, the characteristic times are  $\tau \lesssim 5$  Myr (containing the age grid 0.005 Gyr),  $\sim 5$ –100 Myr (0.025 and 0.10 Gyr), and  $\sim 0.1$ –1 Gyr (0.29, 0.64, and 0.90 Gyr). The large separations ( $\sim 1$ -dex) between these time intervals ensure the recovered SF at different epochs to be well distinguished from one another (e.g., Ocirk et al. 2006). Higher temporal resolution would cause over interpretation due to degeneracies between models with similar ages. The timescales are characteristic of: 1–10 Myr

<sup>1</sup> It is important to include starburst-AGN composites in the analysis because (i) they are a significant population; and (ii) otherwise the sample would be biased against galaxies with high star formation and low AGN activity.

<sup>2</sup> We adopt  $L_{[\text{O III}]}$  uncorrected for extinction and the appropriate calibration rather than the extinction-corrected method because the latter approach is sensitive to uncertainties in the assumed reddening laws and relies on over-simplified dust-screen models (e.g., Reyes et al. 2008).

<sup>3</sup> We caution that the SSFRs in Chen et al. (2009) appear to be inferred using the luminosity coefficients directly without the requisite mass-to-light conversion.

<sup>4</sup> Our results are independent of the specific  $D_n(4000)$  division value chosen in the range of 1.6 to 1.8, but we adopt 1.6 so that the old bulges contain sufficient objects for reliable statistics.

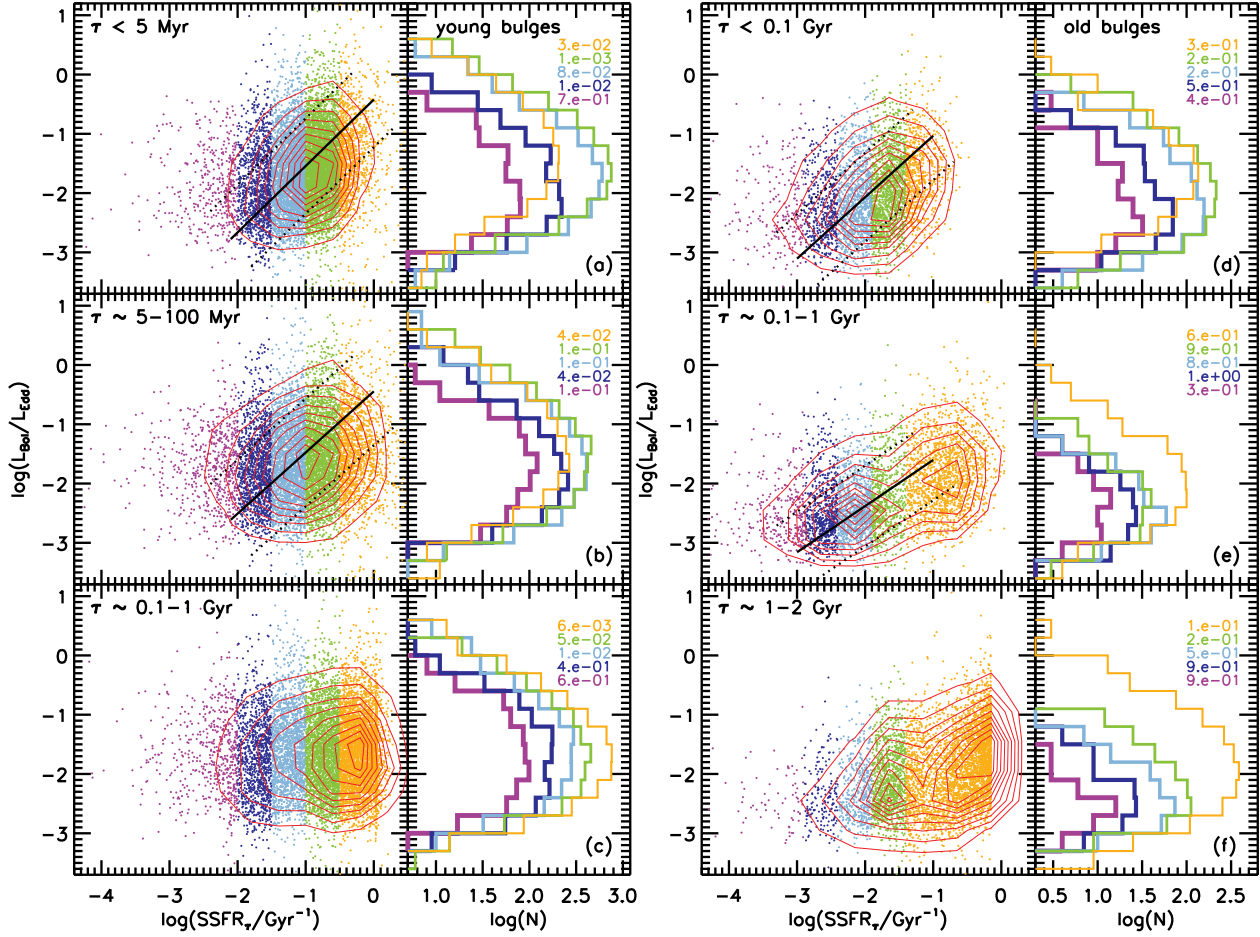


**Figure 1.** Differentiated specific star formation rate ( $\text{SSFR}_\tau$ ) versus Eddington ratio  $\lambda$ . The panels (a)–(c) are for young bulges ( $D_n(4000) < 1.6$ ) whereas the panels (d)–(f) are for old bulges ( $D_n(4000) > 1.6$ ). Look-back time intervals  $\tau$  are labelled on each plot. Data and distribution curves are color coded in  $\text{SSFR}_\tau$  (also discriminated with line thickness). The numbers (also color-coded in  $\text{SSFR}_\tau$ ) are the Kolmogorov-Smirnov (KS) significance denoting the probability that a distribution is normal. Red contours represent ten evenly spaced levels in number density. Black solid and dotted lines show the bisector linear regression fits (median and  $1-\sigma$  uncertainties; Table 1).

for massive star lifetimes (with masses  $\gtrsim 10 M_\odot$ ),  $< 0.1$  Gyr for luminous AGN lifetime (e.g., Yu & Tremaine 2002; Hopkins & Hernquist 2009), and 1–2 Gyr for lifetime of lower-luminosity AGNs (e.g., Hopkins & Hernquist 2009) to which  $D_n(4000)$  is most sensitive to (e.g., Bruzual & Charlot 2003; Kauffmann et al. 2003). For “old” bulges ( $D_n(4000) > 1.6$ ), there is little current SF, and  $\text{SSFR}_\tau$  cannot be reliably estimated for  $\tau \ll 0.1$  Gyr (little mass allowed in the youngest starburst grids). The adopted time intervals are  $\tau \lesssim 0.1$  Gyr (containing the age grids 0.005, 0.025, and 0.10 Gyr),  $\sim 0.1$ –1 Gyr (0.29, 0.64, and 0.90 Gyr), and 1–2 Gyr (1.4 Gyr).

#### 2.4 Uncertainties and Selection Biases

The uncertainty of  $\lambda$  is dominated by the systematics of  $L_{\text{Bol}}$  and  $M_{\text{BH}}$ . The quoted 0.5-dex  $1-\sigma$  uncertainty on  $L_{\text{Bol}}$  contains the intrinsic scatter of the  $L_{[\text{O III}]}$ – $M_{2500}$  relation and the uncertainty of bolometric correction in unobscured AGNs (Liu et al. 2009). For  $M_{\text{BH}}$ , the uncertainty is propagated from  $\sigma_*$  added in quadrature with the 0.3-dex scatter of the  $M_{\text{BH}}$ – $\sigma$  relation (Tremaine et al. 2002). The total  $1-\sigma$  uncertainty of  $\lambda$  is  $\sim 0.6$  dex. We have tested effects of

Malmquist biases due to these scatters, and found that there is little bias on  $M_{\text{BH}}$ , since the  $\sigma_*$  distribution is close to log normal. On the other hand, there is a small yet detectable bias on  $L_{\text{Bol}}$ , such that the inferred  $L_{\text{Bol}}$  is an overestimate (by  $\lesssim 0.03$  dex) of the *true* value (assuming  $L_{\text{Bol}}$  is a prior whereas  $L_{[\text{O III}]}$  is a posterior) given an observed bottom-heavy distribution of  $L_{[\text{O III}]}$  (e.g., Shen et al. 2008).

We have empirically tested the continuum- $\text{SSFR}_\tau$  approach using 12,090 SDSS star-forming galaxies (e.g., Brinchmann et al. 2004). Our initial calibrations were carried out on high-S/N objects (with median S/N  $> 20$  pixel $^{-1}$  and S/N  $> 5$  in  $\sigma_*$ ). To constrain selection biases we tested low-S/N objects using co-added spectra and found similar results. We have verified that  $\text{SSFR}_\tau$  correlate with the current  $\text{SSFR}_e$  using the MPA SFR $_e$  estimates from emission-line modeling (Brinchmann et al. 2004).  $\text{SSFR}_{<5 \text{ Myr}} \approx \text{SSFR}_e$  with a  $1-\sigma$  scatter of  $\sim 0.25$  dex in a bisector fit;  $\text{SSFR}_\tau$  with larger  $\tau$  correlates with but does not equal to the current  $\text{SSFR}_e$ , probably indicating varying SF as a function of look-back time. While these tests are limited to star-forming galaxies, they do lend support to our general approach, especially for young bulges. We take the 0.25-dex scatter as our fiducial estimate for

the  $\text{SSFR}_\tau$  systematic uncertainty. This is comparable to the 0.3-dex estimate from Asari et al. (2007) by comparing continuum-based SFRs against  $\text{H}\alpha$  SFRs for SDSS star-forming galaxies. We have added noise to spectra of a randomly selected subsample, and found that typical errors of SSFRs due to noise in the continuum spectra are no larger than  $\sim 0.2$  dex. We take 0.3 dex as our fiducial estimate for the total  $1\text{-}\sigma$  uncertainty for  $\text{SSFR}_\tau$ .

### 3 RESULTS

Fig. 1 shows Eddington ratio ( $\lambda$ ) versus  $\text{SSFR}_\tau$ , and the  $\lambda$  distribution ( $P(\log\lambda)$ ) as a function of  $\text{SSFR}_\tau$ . The young bulges ( $D_n(4000) < 1.6$ ) have median  $\log(L_{[\text{O III}]} / L_\odot) = 6.89$  (with a  $1\text{-}\sigma$  scatter of 0.39 dex) and  $\log(M_*/M_\odot) = 10.88 (\pm 0.32)$ , whereas the old bulges ( $D_n(4000) > 1.6$ ) have median  $\log(L_{[\text{O III}]} / L_\odot) = 6.73 (\pm 0.35)$  and  $\log(M_*/M_\odot) = 11.13 (\pm 0.33)$ . For  $\tau \leq \tau_0$  ( $\tau_0 \sim 0.1$  Gyr for young and  $\sim 1$  Gyr for old bulges), both populations appear to follow power laws. The correlations are strong: the Spearman probabilities for null correlation are close to zero (Table 1, Col. 8); the relations flatten out when  $\tau \gtrsim \tau_0$  (Table 1, Col. 7). The cutoff in Fig. 1f at the high  $\text{SSFR}_\tau$  end is artificial due to its definition and the limited temporal resolution of the continuum approach<sup>5</sup>.

#### 3.1 The $\lambda$ -SSFR Relation

$\lambda$  of AGNs in young bulges correlate with their current SSFRs ( $\text{SSFR}_{\tau < 5\text{Myr}}$ ; Fig. 1a). We fit the relation  $\lambda = 10^b(\text{SSFR}/\text{Gyr}^{-1})^k$ , the linear regression results of which are given in Table 1 in. We adopt bisector fits appropriate for two variables with no assumption of one depending on another. The fit for young bulges is  $\log\lambda = (-0.42 \pm 0.01) + (1.12 \pm 0.01)\log(\text{SSFR}/\text{Gyr}^{-1})$ . The scatter ( $1\text{-}\sigma$  orthogonal of 0.54 dex) is dominated by observational uncertainties. Given any fixed  $\text{SSFR}_\tau$ ,  $P(\lambda)$  is roughly log normal, and its central value increases with increasing  $\text{SSFR}_\tau$ . While some of the Kolmogorov-Smirnov (KS) probabilities labelled in Fig. 1 are small, when we divide the sample into finer bins in  $\text{SSFR}_\tau$  the KS probabilities become larger.

In old bulges with measurable SSFRs,  $\lambda$  also correlates with recent SSFRs ( $\text{SSFR}_{\tau < 0.1\text{Gyr}}$ ; Fig. 1d). The fit for old bulges is  $\log\lambda = (0.00 \pm 0.01) + (1.00 \pm 0.01)\log(\text{SSFR}/\text{Gyr}^{-1})$  (Table 1). Considering uncertainties, this is similar to the relation in young bulges, although the median  $\lambda$  is  $\sim 1$  dex smaller than in young bulges. Similarly, given any fixed  $\text{SSFR}_\tau$ ,  $P(\lambda)$  is close to log normal, and the central  $\lambda$  increases with increasing  $\text{SSFR}_\tau$ .

<sup>5</sup> The cutoff is reached if all mass is recovered in the 1.4 Gyr grid. In practice this only happens for  $\tau > 1$  Gyr. For younger ages, the cutoff is never reached, because while most of the light may go into young populations, it is always the old populations which dominates the *total* mass (due to the drastically different mass-to-light ratios of old and young stars).

**Table 1.** Results of the fits  $\log(\lambda) = b + k \log(\text{SSFR}_\tau/\text{Gyr}^{-1})$

Sample (1)	$\tau/\text{Gyr}$ (2)	$b$ (3)	$k$ (4)	$\sigma$ (5)	N (6)	$\rho$ (7)	$P_{\text{null}}$ (8)
young	$\leq 0.005$	-0.42	1.12	0.54	9903	0.23	$< 10^{-40}$
young	0.005–0.1	-0.45	1.03	0.63	8420	0.15	$< 10^{-40}$
young	0.1–1	-0.81	1.00	0.68	9951	0.01	0.5
old	$\leq 0.1$	0.00	1.00	0.52	3921	0.29	$< 10^{-40}$
old	0.1–1	-0.82	0.78	0.54	4302	0.29	$< 10^{-40}$
old	1–2 <sup>‡</sup>	-0.37	1.04	0.48	5351	0.16	$10^{-16}$

Col. (1):  $D_n(4000) < 1.6$  for “young” whereas  $D_n(4000) > 1.6$  for “old” bulges; Col. (2): look-back time  $\tau$ ; Cols. (3) & (4): normalization and slope from the bisector fits with  $1\text{-}\sigma$  uncertainties of  $\lesssim 0.01$  dex; Col. (5): standard deviation of the distribution.  $\sigma$  is measured along the orthogonal direction to the fit; Col. (6): number of objects in each subsample. To be included, a galaxy needs to contain mass in at least one of the starburst grids in interval  $\tau$ ; Cols. (7) & (8): Spearman correlation test coefficients. <sup>‡</sup> For Fig. 1f, the fits are for 2499 objects with  $\log(\text{SSFR}/\text{Gyr}^{-1}) < -1$ , to minimize effects from the artificial cutoff at the high SSFR end.

#### 3.2 Correlation between AGN Activity and Recent Bulge Star Formation

In young bulges  $\lambda$  also correlates with SSFRs averaged over the past  $\sim 5\text{--}100$  Myr (Fig. 1b). The correlation for  $\tau \sim 5\text{--}100$  Myr is similar to  $\tau \sim 5$  Myr (Table 1). For young bulges, the correlation flattens out when  $\tau \sim 0.1\text{--}1$  Gyr (Fig. 1c): given a fixed  $\text{SSFR}_\tau$ ,  $P(\lambda)$  is still largely log normal, yet  $\lambda$  depends little on  $\text{SSFR}_\tau$  averaged over the past  $\sim 0.1\text{--}1$  Gyr. Figs. 1(e,f) show similar results in old bulges with the main difference of having a larger  $\tau_0$  ( $\sim 1$  Gyr). While there is still some correlation for  $\tau \sim 1\text{--}2$  Gyr (Figs. 1f) partially due to the artificial cutoff, the relation starts to flatten out (Spearman  $\rho$  being smaller; Table 1).

### 4 DISCUSSION

Our results imply similar relations between AGN activity and recent SF in old and young bulges, despite different Eddington ratios observed. The current Eddington ratio correlates with the most recent bulge SF:  $\lambda \propto \text{SSFR}_\tau$  estimated in a certain look-back time interval  $\tau$ ; it depends little on SF happened before some threshold time  $\tau_0$ . The main difference between young and old bulges is on  $\tau_0$ : young bulges have  $\sim 0.1$  Gyr whereas old bulges have  $\sim 1$  Gyr.

Recently Kauffmann & Heckman (2009) have studied the  $\lambda$  distribution as a function of  $D_n(4000)$ . These authors find that  $P(\lambda)$  is log normal in young bulges and exponential in old bulges, and suggest two growth regimes. While this could still be the case, Hopkins & Hernquist (2009) suggest that different  $\lambda$  distributions may also arise from universal AGN light curves with different quench times: AGNs in old bulges have apparent exponential  $P(\lambda)$  because accretion and star formation were quenched in a series of earlier epochs (see also e.g., Shen 2009). Our results point to the latter explanation. Namely, the physical processes that link AGN activity and bulge SF seem to work universally in young and old bulges, albeit with different quenching/threshold times.

Using population synthesis analysis, we have found that when grouped in terms of similar SF activity with ages less than typical AGN lifetimes, BHs in old bulges also have log

normal  $P(\lambda)$ . We have shown that for BHs in young bulges,  $\lambda$  does correlate with the most recent SF (Figs. 1a,b). The reason why Kauffmann & Heckman (2009) found little correlation is most likely that the temporal resolution of  $D_n(4000)$  is not enough to disintegrate the most recent SF in young bulges. The reciprocal  $\text{SSFR}_\tau^{-1}$ , which is the mass-weighted stellar age averaged among the stellar populations formed over  $\tau$ , can be estimated for different timescales  $\tau$ , whereas  $D_n(4000)$  is most sensitive to  $\tau = 1\text{--}2$  Gyr. If we assume the observed sample consists of AGNs at different evolutionary stages, the  $\lambda$ -SSFR results (Table 1) imply light curves  $\lambda \propto t^{-(1.0-1.1)}$ , which is noticeably less steep than predictions  $\lambda \propto t^{-(1.5-2.0)}$  from models assuming extreme gas expel by AGNs (e.g., Hopkins & Hernquist 2009). This milder decay could suggest more moderate self-regulated AGN and SF activity, although the observational uncertainties in our results are significant.

Another implication is that AGN environmental studies should draw control samples matched not only in the mean stellar age (as usually implemented using  $D_n(4000)$ ), but also in the most recent bulge SF properties. The effect would be particularly important for AGNs in young bulges, as we have shown that their SF-AGN-correlation timescale is usually much shorter ( $\sim 0.1$  Gyr) than that probed by the overall mean stellar age.

Our results are limited to optical AGNs with  $\bar{z} \sim 0.1$  and  $L_{\text{Bol}} \sim 10^{43}\text{--}10^{45}$  erg s $^{-1}$ , and may not apply to other AGN populations. In principle the approach could be extended to lower-luminosity AGNs (LINERs) and to higher-luminosity AGNs and quasars, although selection incompleteness and biases may be more severe. Multi-wavelength SFR indicators that probe different SF timescales or phases may also help elucidate the AGN-SF relation as a function of look-back time. The approach demonstrated based on population synthesis analysis relies on statistical AGN samples with high-S/N spectra. We look forward to the next generation of ground-based near-IR multi-object spectrographs (e.g., Bell, et al. 2010) that will make an equivalent study possible at high redshifts to better understand the coupled growths of stellar bulges and SMBHs in the early universe.

## ACKNOWLEDGMENTS

I am grateful to my thesis advisor M. Strauss for his generous encouragement and for comments on the manuscript. I also acknowledge Y. Shen and J. Gunn for helpful discussion on selection biases, and an anonymous referee for a careful and useful report. Funding for the SDSS and SDSS-II has been provided by the Alfred P. Sloan Foundation, the Participating Institutions, the National Science Foundation, the U.S. Department of Energy, the National Aeronautics and Space Administration, the Japanese Monbukagakusho, the Max Planck Society, and the Higher Education Funding Council for England. The SDSS Web Site is <http://www.sdss.org/>. Facilities: Sloan

## REFERENCES

- Adelman-McCarthy J. K., et al., 2008, *ApJS*, 175, 297  
 Antonucci R., 1993, *ARA&A*, 31, 473  
 Asari N. V., et al., 2007, *MNRAS*, 381, 263  
 Baldwin J. A., Phillips M. M., Terlevich R., 1981, *PASP*, 93, 5  
 Balogh M. L., Morris S. L., Yee H. K. C., Carlberg R. G., Ellingson E., 1999, *ApJ*, 527, 54  
 Begelman M. C., Cioffi D. F., 1989, *ApJL*, 345, L21  
 Bell E., et al., 2010, *The Astronomy and Astrophysics Decadal Survey*, 2010, 106  
 Bica E., 1988, *A&A*, 195, 76  
 Binney J., 1977, *ApJ*, 215, 483  
 Boroson T. A., Oke J. B., 1982, *Nature*, 296, 397  
 Brinchmann J., Charlot S., White S. D. M., Tremonti C., Kauffmann G., Heckman T., Brinkmann J., 2004, *MNRAS*, 351, 1151  
 Bruzual G., 1983, *ApJ*, 273, 105  
 Bruzual G., Charlot S., 2003, *MNRAS*, 344, 1000  
 Burkert A., Silk J., 2001, *ApJL*, 554, L151  
 Canalizo G., Stockton A., 2000, *ApJ*, 528, 201  
 Chen, Y.-M., Wang, J.-M., Yan, C.-S., Hu, C., Zhang, S., 2009, *ApJL*, 695, 130  
 Cid Fernandes R., et al., 2004, *MNRAS*, 355, 273  
 Cid Fernandes R., Mateus A., Sodré L., Stasińska G., Gomes J. M., 2005, *MNRAS*, 358, 363  
 Ciotti L., Ostriker J. P., 1997, *ApJL*, 487, L105+  
 Fabian A. C., 1999, *MNRAS*, 308, L39  
 Ferrarese L., Merritt D., 2000, *ApJL*, 539, L9  
 Gebhardt K., et al., 2000, *ApJL*, 539, L13  
 Greene J. E., Zakamska N. L., Liu X., Barth A. J., Ho L. C., 2009, *ApJ*, 702, 441  
 Heckman T. M., 2009, *Astrophysics and Space Science Proceedings*, Volume. ISBN 978-1-4020-9456-9, p. 335  
 Heckman T. M., Kauffmann G., Brinchmann J., Charlot S., Tremonti C., White S. D. M., 2004, *ApJ*, 613, 109  
 Hopkins P. F., Hernquist L., 2009, *ApJ*, 698, 1550  
 Jahnke K., Wisotzki L., Courbin F., Letawe G., 2007, *MNRAS*, 378, 23  
 Kauffmann G., Heckman T. M., 2009, *MNRAS*, 397, 135  
 Kauffmann G., et al., 2003, *MNRAS*, 346, 1055  
 Kewley L. J., Dopita M. A., Sutherland R. S., Heisler C. A., Trevena J., 2001, *ApJ*, 556, 121  
 Liu X., Zakamska N. L., Greene J. E., Strauss M. A., Krolik J. H., Heckman T. M., 2009, *ApJ*, 702, 1098  
 Moore B., Katz N., Lake G., Dressler A., Oemler A., 1996, *Nature*, 379, 613  
 Netzer H., 2009, *MNRAS*, 399, 1907  
 Norman C., Scoville N., 1988, *ApJ*, 332, 124  
 Ocvirk P., Pichon C., Lançon A., Thiébaud E., 2006, *MNRAS*, 365, 46  
 Rees M. J., Ostriker J. P., 1977, *MNRAS*, 179, 541  
 Reyes R., et al., 2008, *AJ*, 136, 2373  
 Sanders D. B., Soifer B. T., Elias J. H., Madore B. F., Matthews K., Neugebauer G., Scoville N. Z., 1988, *ApJ*, 325, 74  
 Silk J., Norman C., 2009, *ApJ*, 700, 262  
 Silk J., Rees M. J., 1998, *A&A*, 331, L1  
 Shen Y., Greene J. E., Strauss M. A., Richards G. T., Schneider D. P., 2008, *ApJ*, 680, 169  
 Shen Y., 2009, *ApJ*, 704, 89  
 Springel V., Di Matteo T., Hernquist L., 2005, *MNRAS*, 361, 776  
 Tremaine S., et al., 2002, *ApJ*, 574, 740  
 Tremonti C. A., et al., 2004, *ApJ*, 613, 898  
 Urry C. M., Padovani P., 1995, *PASP*, 107, 803  
 York D. G., et al., 2000, *AJ*, 120, 1579  
 Yu Q., Tremaine S., 2002, *MNRAS*, 335, 965  
 Zakamska N. L., et al., 2006, *AJ*, 132, 1496